Arabian Journal for Science and Engineering
https://doi.org/10.1007/s13369-021-05627-2

RESEARCH ARTICLE-MECHANICAL ENGINEERING

Development of a Generalized Mathematical Model for Slider-Crank Mechanism Based on Multiobjective Concurrent Engineering with Application

Hoang Minh Dang[1] · Van Phuong Bui[2] · Van Binh Phung[3] · Do Van Thom[3] · Phung Van Minh[3] · Sergey Sergeevich Gavriushin[2,4] · Nguyen Viet Duc[5]

Received: 6 January 2021 / Accepted: 30 March 2021

Abstract
A design optimization of a slider-crank mechanism (SCM) based upon multiobjective concurrent engineering is presented in this paper. The proposed generalized mathematical model includes geometric equations, kinetic–dynamic expressions, fatigue strength and stability requirements and allows to take into consideration the manufacturing capabilities available. The model also allows for describing the actual mechanism characteristics and can be used directly for the detailed design stage of SCMs, in contrast to the simplified physical models available for preliminary design. Based on this approach, the multiobjective model of SCM which includes 11 variables, seven constrained expressions and the three most important objective functions (total mass, required power and maximum dynamic reaction) was developed. The closed-form analytical expressions were established to the relationship between objective functions, constraints and variables. The correctness of the model was checked by using the finite element method. By using the developed model, the optimization design of the main transmission of a fruit/vegetable washer was carried out. The genetic algorithm optimization has yielded 73 Pareto optimal solutions, and the three most suitable solutions according to the specific manufacturing capability were determined by employing a decision-making process based on the method of successive concessions. Further, a comparative study showed that the solutions obtained by the developed model have excelled the one obtained by means of the experience-based approach. It is noteworthy that the generalized mathematical model and the problem-solving approach adopted in this work can also be used for the SCM synthesis of other mechanical systems.

Keywords Slider-crank mechanism synthesis · Multiobjective optimization model · Concurrent engineering · Decision-making process · Genetic algorithm optimization · Fruit vegetable washer

1 Introduction

Slider-crank mechanism (SCM) has been widely used in different kinds of devices [1]. However, the design of SCMs is still is a complex issue that has drawn the attention of many researchers [2, 3]. To this end, the design of a mechanical device is traditionally divided into several steps, as it can be observed in Fig. 1a. Once a preliminary design had been reached, it could be modelled in a three-dimensional coordinate system (3D), and then the kinematic–dynamic analysis could be properly examined. After that, the strength of every structural element, which refers to the most important link of SCM such as a crank or a connecting rod (or conrod, for short), is verified. If the design option is suitable, it will be used for the manufacturing process, otherwise the 3D model configuration needs to be rectified. For this purpose, this

✉ Nguyen Viet Duc
ducnv@tlu.edu.vn

1 Industrial University of Ho Chi Minh City, Ho Chi Minh City, Vietnam

2 Bauman Moscow State Technical University, Moscow, Russian Federation

3 Le Quy Don Technical University, Hanoi, Vietnam

4 Mechanical Engineering Research Institute of the Russian Academy of Sciences, Moscow, Russian Federation

5 Thuyloi University, 175 Tay Son, Dong Da, Hanoi, Vietnam

Published online: 22 April 2021

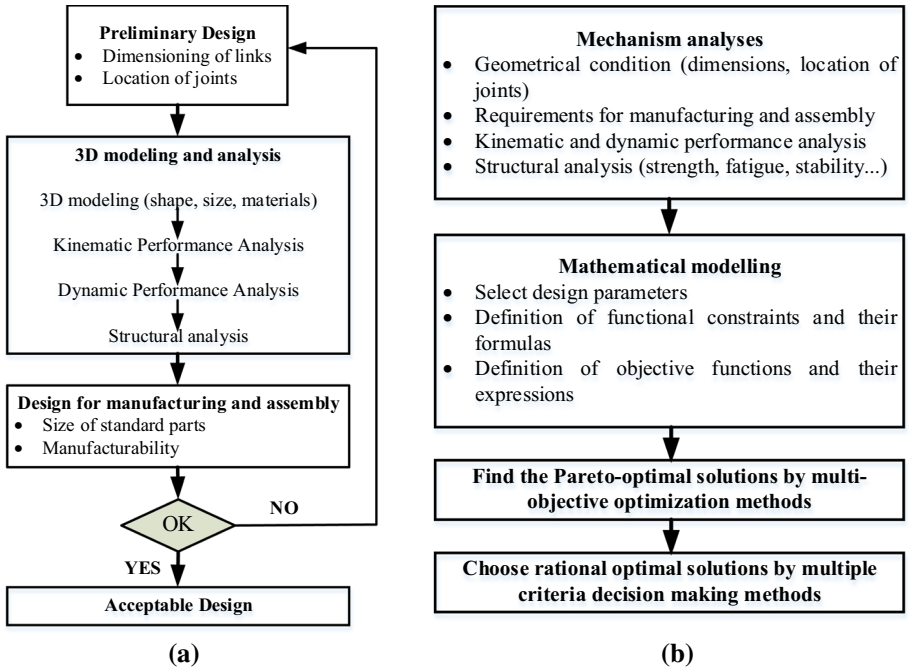

Fig. 1 Design process of slider-crank mechanism. **a** Traditional approach; **b** Proposed approach

process is usually carried out by means of computer-aided design (CAD) software, in which for every design option the calculation is performed by manually shifting over different computing modules to check the corresponding requirements. However, the calculation process has to be carried out repeatedly until a valid solution is reached, which is both costly and time-consuming [4]. It is thus evident that only a small number of solutions are ordinarily analysed. The selected one sometimes depends on the subjective evaluation of a design engineer instead of the actual optimal one for the case.

Although there are numerous publications regarding design optimization of SCMs, most of them have concentrated on several particular features rather than the development of a generalized mathematical model. For instance, Refs. [5, 6] are only concerned about equations describing the boundary geometry and kinetics of SCM. Also, the dynamics of SCMs are studied in Refs. [7, 8], while the structural equilibrium of SCMs is analysed in Refs. [9, 10].

In Ref. [11], the dynamics of SCMs is analysed taking into account the effect of joint clearances. Further, Refs. [12, 13] explored the influence of both flexible components and joint clearance on the dynamics of SCMs. Besides, it is noteworthy that in many multiobjective mathematical models presented in the published works many important factors were either simplified or omitted. As an example, the models of Khemili et al. [14] and Mariti et al. [15] only involved kinetics and dynamics of SCMs, but shape and dimension of the structural elements (crank and conrod) were not taken into consideration. In contrast to this, the shape of the crank and the conrod was studied in the models of Azegami et al. [16] and of Chaudhary [17], but manufacturability and strength requirements were not considered. Equally important, the mathematical sub-models were also drastically simplified, i.e. for kinematic analysis, only the dimension of structural elements was considered, leaving out of the analysis its shape and mass. While dealing with dynamics, several structural element features, such as weight, moment of inertia and gravity centre, were taken into account in [18], but its shape and s0tiffness were disregarded. (The links were assumed to be a rigid body).

With respect to the detailed design of the crank and the conrod, Ref. [19] presented a mathematical model, in which the exerted load on the system was given as an input datum, with a constant magnitude, while dynamic factors were ignored. This means that most of published works concentrated mainly on calculations for preliminary design stages [20], and the solution obtained from the optimization problem only served as guidelines or recommendations, rather than being directly useful for manufacturing purposes. Yet, most of developed multiobjective models have simplified physical forms and overlooked the features of a real structure such as strength, shapes and sizes suitable for the manufacturing facilities available.

As a result of this, the whole design process of SCMs still follows the traditional approach, as shown in Fig. 1a. To overcome the limitations of traditional approaches, a new one is proposed in this paper, i.e. an approach based on multiobjective concurrent engineering [21, 22] as shown in Fig. 1b. The essence of this approach is the development of a generalized mathematical model for SCM analyses. This new model takes into account numerous requirements

at different design stages. Apart from the features that belong to the traditional approach, such as geometrical and kinetic–dynamic characteristics, SCM strength and stability requirements, manufacturability is included in the generalized mathematical model. This model can be directly implemented for the detailed design of SCMs. Accordingly, the model allows for the automatic calculation of kinematic (trajectory, velocity, acceleration) and dynamic (support reaction, torque) variables, as well as structural strength, stability and fatigue analyses of SCMs. With this model, numerous design solutions can be quickly analysed. The optimization algorithm, i.e. the genetic algorithm, is used for the determination of the set of Pareto optimal solutions. Some reasonable solutions are then selected with the aid of a decision-making method. As an example, this process was used for the fabrication of fruit/vegetable washer main transmission [23, 24].

The rest of this paper is organized as follows. Section 2 presents a generalized mathematical model, in which the geometric, kinematic and dynamic equations, structural characteristics, manufacturability and assembly condition are fully described. The generalized mathematical model and validation of the model are presented in Sect. 3. Section 4 introduces the determination of Pareto optimal solutions as well as the filter of solutions with the multiobjective decision-making method. Then, the results and discussions are figured out. Section 5 concludes some novelty contributions of this work.

2 Generalized Mathematical Model

The configuration of an SCM is determined by seeking to comply with space limitations and geometrical restrictions in order to avoid possible singularities. The shape and the dimensions of structural elements are selected on the basis of standardized elements and manufacturability. Kinematic and dynamic equations are set to describe the performance of the mechanism. Besides, strength and stability equations are developed to ensure safety and reliability for the whole structure. SCMs are analysed as schematically shown in Fig. 2.

2.1 Geometric Equations

In the design of SCMs, the first problem that as to be faced is its adequate location, as shown in Fig. 3. Also, the whole device should be bounded by outer working space

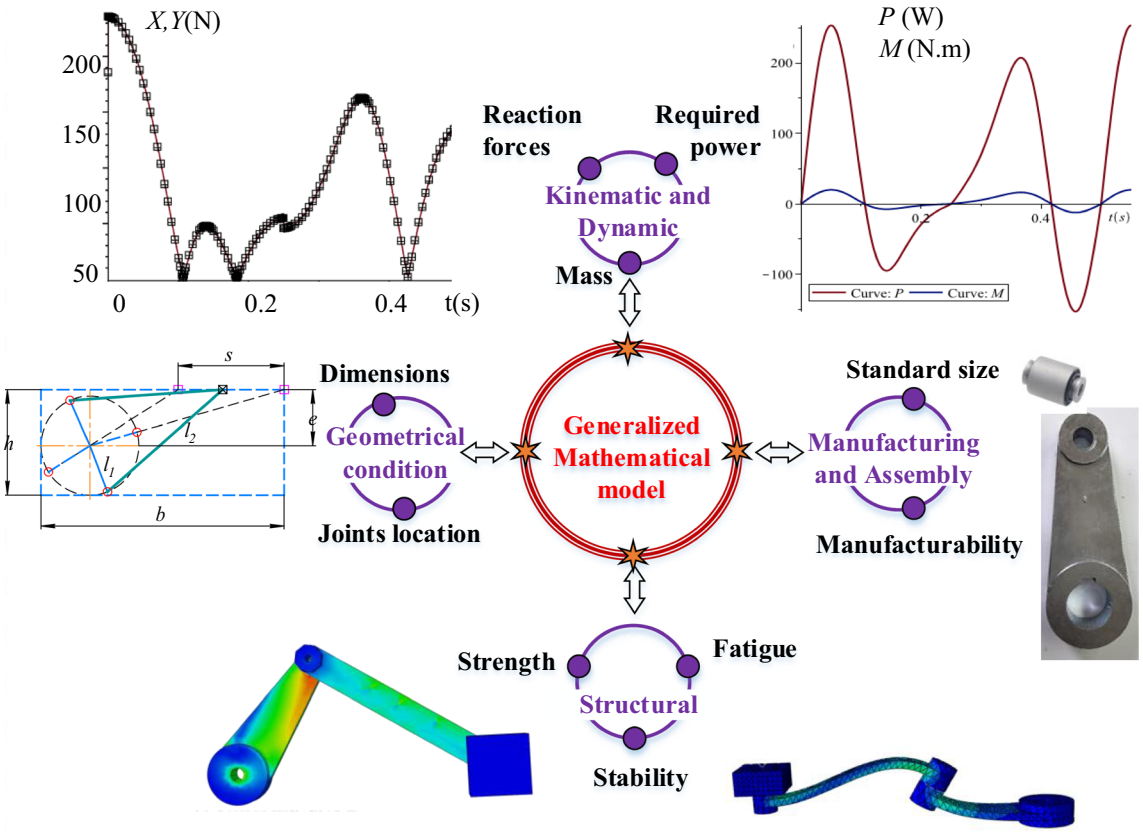

Fig. 2 Schematic overview of the analysis process

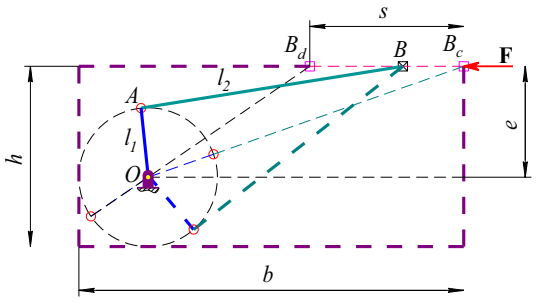

Fig. 3 Schematic representation of an SCM, where the trajectory s lays on the line B_d-B_c, with B_d being the starting point and B_c the end of the stroke

dimensions h and b and its slider undergoes a resistive force F. Hence, to synthesize an SCM, it is necessary to define lengths l_1 and l_2, as well as eccentricity e that conform to the working space limitation. In order to comply with these requirements, it is possible to analyse one of the two systems of equations, each corresponding, to a specific situation, as depicted in Fig. 4.

Should the groove with length s fall beyond the radius of the crank, Fig. 4a, geometrical constraints are included in the system of Eq. 1.

$$\begin{cases} \sqrt{(l_2+l_1)^2-e^2}-\sqrt{(l_2-l_1)^2-e^2}=s \\ l_1+\sqrt{(l_2+l_1)^2-e^2}=b \\ l_1+e=h \\ l_1>0 \\ l_2\geq l_1+e=h \\ e>l_1 \end{cases} \tag{1}$$

On the other hand, if the groove/sliding link falls within the crank circle, Fig. 4b, the geometrical constraints are included in the system of Eq. 2

$$\begin{cases} \sqrt{(l_2+l_1)^2-e^2}-\sqrt{(l_2-l_1)^2-e^2}=s \\ l_1+\sqrt{(l_2+l_1)^2-e^2}=b \\ 2l_1=h \\ l_1>0 \\ l_2\geq l_1+e=\dfrac{h}{2}+e \\ e\leq l_1 \end{cases} \tag{2}$$

If s and h were equal, the second design option will bring an in-line SCM, and then $e=0$, $l_1=h/2$, $l_2=b–h$, while if $s<h$, only the first design option is suitable, otherwise, if $s\geq h$, it is possible to use both solutions. Although the first set of equations would provide a more effective solution, the total length of bars (l_1+l_2) would be greater, thereby resulting in larger dynamic forces being generated.

2.2 Manufacturability and Assembly Condition

Shapes of the crank and the conrod are determined on the basis of manufacturability and assembly condition [16, 17]. Links are usually symmetrical, with dimensions depicted as in Fig. 5.

Bushing housing diameters d_1 and d_2 are selected from standard bushing sizes, while dimensions of the key are h_t, b_t and t_t.

The following expression (3) provides additional dimensional conditions so that the crank can rotate freely, where Δi, $i=1\ldots4$ are safety excesses.

$$\begin{cases} h_1\geq t_1+\Delta_1 \\ h_2\geq t_1+\Delta_2 \\ h_3\geq t_2+\Delta_3 \\ h_2+h_3\geq h_1+t_2+\Delta_4 \end{cases} \tag{3}$$

Further, there are conditions regarding manufacturability and requirements for assembly, which are set forth in expression (4), where Δi, $i=5\ldots8$ are safety excesses.

Fig. 4 Two distinct SCMs situations

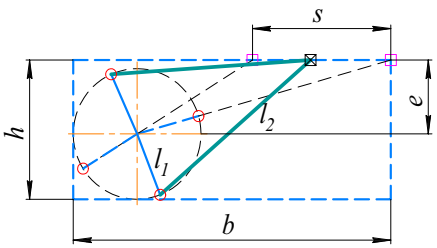

(a) Situation 1

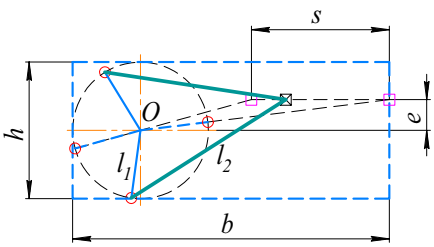

(b) Situation 2

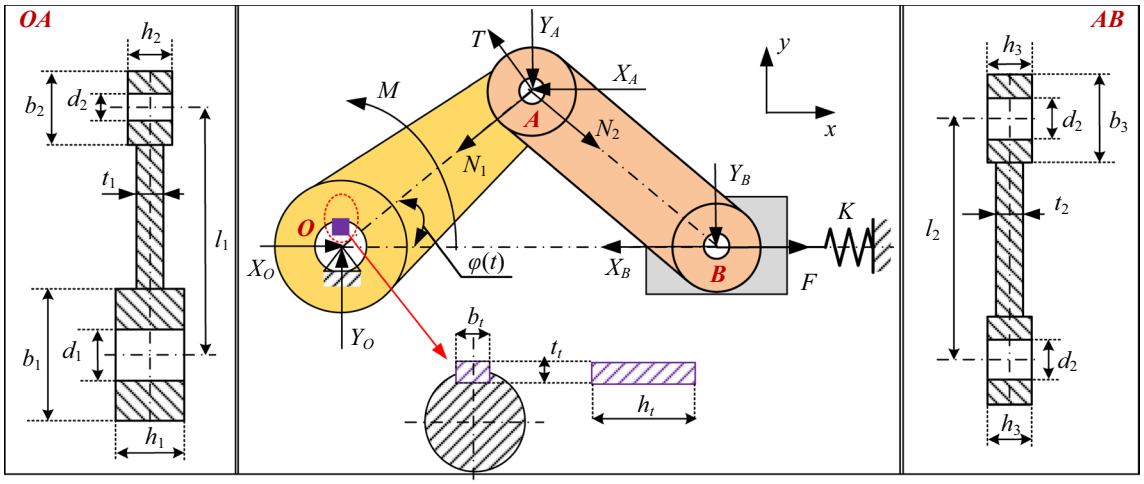

Fig. 5 Selected configuration of the crank and the conrod in accordance with fabrication technology

$$\begin{cases} b_1 \geq d_1 + \Delta_5 \\ b_2 \geq d_2 + \Delta_6 \\ b_3 \geq d_2 + \Delta_7 \\ \dfrac{b_1}{b_2} \geq \Delta_8 \end{cases} \tag{4}$$

2.3 Kinematic and Dynamic Models

To reduce shaking force, a spring is attached to the SCM (spring-SCM), rather than using counterweights [9]. This prevents the increase of mass, size and volume of the structure, and the spring-SCM system will turn into the traditional SCM if spring stiffness K is null. The calculation scheme for kinematic and dynamic analysis of the spring-SCM system under a single force F is illustrated in Fig. 6.

Friction at the joints is assumed negligible. The segment OA (crank) and AB (connecting rod) possess length l_1 and l_2, mass m_1 and m_2, gravity centre C and G, respectively. The slider B, which has mass m_3, slides in the groove with an eccentricity e from the O-axis of the motor. The slider B is impelled by the external force F, consisting of the drag force F_c and the spring force. The dynamics of an SCM can be solved by using D´Alambert´s principle [25]. To build the model for the SCM, support reactions at joint O (X_O, Y_O), joint A (X_A, Y_A), joint B (X_B, Y_B), and reaction N_B at the slider B are considered as well as the required power P, which is obtained on the basis of moment M of the motor and angular velocity $\omega = \frac{\partial \varphi}{\partial t}$ at the joint O of the segment OA.

Dynamic reaction at joint O:

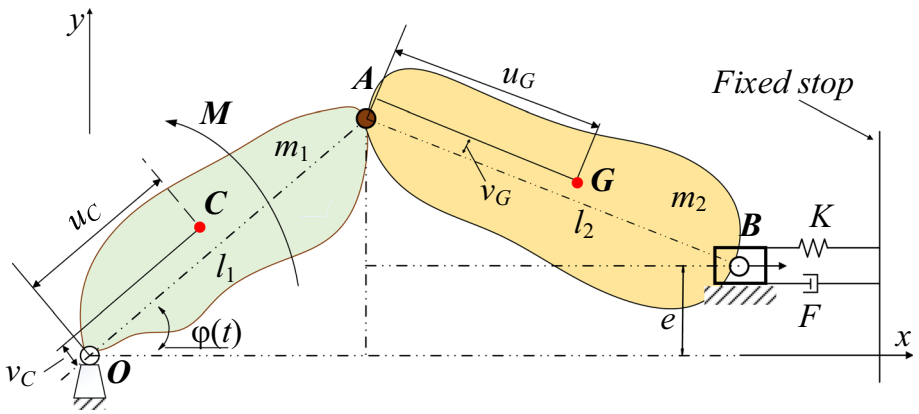

Fig. 6 Scheme for kinematic and dynamic analysis of a spring-SCM system

$$X_O = \frac{-(x_A - x_B)}{x_A - x_B + s\mu(y_A - y_B)} F + m_1 a_{Cx} + \frac{-1}{x_A - x_B + s\mu(y_A - y_B)} \left[s\mu I_{Gz} \varepsilon_{\mathrm{AB}} \right. \\ \left. -(x_A - x_B)(m_3(g\mu s + a_B) + m_2 a_{Gx}) - s\mu m_2((a_{Gy} + g)(x_A - x_G) - a_{Gx}(y_B - y_G)) \right] \tag{5}$$

Drag force F can be derived as follows:

$$Y_O = \frac{-(y_A - y_B)}{x_A - x_B + s\mu(y_A - y_B)} F + m_1(a_{Cy} + g) + \frac{-1}{x_A - x_B + s\mu(y_A - y_B)} \left[-I_{Gz} \varepsilon_{\mathrm{AB}} \right. \\ \left. -m_2(a_{Gx}(y_A - y_G) - (a_{Gy} + g)(x_B - x_G)) - (y_A - y_B)(m_2 \mu s(a_{Gy} + g) + m_3(\mu s g + a_B)) \right] \tag{6}$$

$$F = -K(x_B - l_2) - s \cdot F_c - s \cdot \mu \cdot N_B \tag{12}$$

Dynamic reaction at joint A:

$$X_A = \frac{(x_A - x_B)}{x_A - x_B + s\mu(y_A - y_B)} F + \frac{1}{x_A - x_B + s\mu(y_A - y_B)} \left[s\mu I_{Gz} \varepsilon_{\mathrm{AB}} \right. \\ \left. -(x_A - x_B)(m_3(g\mu s + a_B) + m_2 a_{Gx}) - s\mu m_2((a_{Gy} + g)(x_A - x_G) - a_{Gx}(y_B - y_G)) \right] \tag{7}$$

$$Y_A = \frac{y_A - y_B}{x_A - x_B + s\mu(y_A - y_B)} F + \frac{1}{x_A - x_B + s\mu(y_A - y_B)} \left[-I_{Gz} \varepsilon_{\mathrm{AB}} \right. \\ \left. -m_2(a_{Gx}(y_A - y_G) - (a_{Gy} + g)(x_B - x_G)) - (y_A - y_B)(m_2 \mu s(a_{Gy} + g) + m_3(\mu s g + a_B)) \right] \tag{8}$$

Dynamic reaction at joint B:

$$X_B = \frac{(x_A - x_B)}{x_A - x_B + s\mu(y_A - y_B)} F + \frac{1}{x_A - x_B + s\mu(y_A - y_B)} \left[s\mu I_{Gz} \varepsilon_{\mathrm{AB}} \right. \\ \left. -m_3(x_A - x_B)(g\mu s + a_B) - s\mu m_2((a_{Gy} + g)(x_A - x_G) - a_{Gx}(y_A - y_G)) \right] \tag{9}$$

$$Y_B = \frac{y_A - y_B}{x_A - x_B + s\mu(y_A - y_B)} F + \frac{1}{x_A - x_B + s\mu(y_A - y_B)} \left[-I_{Gz} \varepsilon_{\mathrm{AB}} \right. \\ \left. -m_2(a_{Gx}(y_A - y_G) - (a_{Gy} + g)(x_A - x_G)) - m_3(y_A - y_B)(\mu s g + a_B) \right] \tag{10}$$

Required driving power:

$$P = \omega \cdot \left[\frac{x_A y_B - x_B y_A}{x_A - x_B + s\mu(y_A - y_B)} F + \frac{1}{x_A - x_B + s\mu(y_A - y_B)} \left[(x_A + s\mu y_A)(I_{Gz} \varepsilon_{AB} - m_2 a_{Gx} y_G) \right. \right. \\ -m_2(a_{Gy} + g)(x_A(x_B + s\mu y_B) - x_G(x_A + s\mu y_A)) - m_3(x_A y_B - x_B y_A)(g s\mu + a_B) \\ \left. \left. (-m_2 a_{Gx} y_A(x_B + s\mu y_B)) \right] + I_{Cz} \varepsilon + m_1(x_C(a_{Cy} + g) - y_C a_{Cx}) \right] \tag{11}$$

where μ is an average coefficient of friction between the slider and the groove.

Dynamic reaction at joint B is obtained by the following formula:

$$N_B = -\frac{(y_A - y_B)\left[K(x_B - l_2) + s \cdot F_c\right]}{x_A - x_B + s \cdot 2\mu(y_A - y_B)} + \frac{1}{x_A - x_B + s \cdot 2\mu(y_A - y_B)}\left[-I_{Gz}\epsilon_{AB} + \right.$$
$$\left. -m_2\left(a_{Gx}(y_A - y_G) - (a_{Gy} + g)(x_A - x_G)\right) - m_3\left(a_B(y_A - y_B) - g(x_A - x_B)\right)\right] \tag{13}$$

with the kinetic features being provided in detail in Appendix 1.

For convenience, the analytical expressions describing geometrical features, mass and moment of inertia of the crank and the conrod are build based on the geometrical parameters of the structure [26]. Coordinates of gravity centres of the crank (u_C) and conrod (u_G) are given by:

$$\begin{cases} u_C = \dfrac{\sum\limits_i zC_i V_i^{CS}}{\sum\limits_i V_i^{CS}} - \dfrac{b_1}{2} \\ u_G = \dfrac{l_2}{2} \end{cases} \tag{14}$$

while the moments of inertia corresponding to gravity centres of the crank (I_{Cz}) and the conrod (I_{Gz}) can be determined from:

$$\begin{cases} I_{Cz} = \sum\limits_i I_{C_i}^{YY} + \sum\limits_i m_i^{CS} r_{CC_i}^2 \\ I_{Gz} = \sum\limits_j I_{G_i}^{YY} + \sum\limits_j m_j^{CR} r_{GG_j}^2 \end{cases} \tag{15}$$

Mass of the crank and the conrod and the entire structure are given by:

$$\begin{cases} m_1 = \rho \sum\limits_i V_i^{CS} \\ m_2 = \rho \sum\limits_j V_i^{CR} \\ m = m_1 + m_2 \end{cases} \tag{16}$$

where z_{Ci} is the coordinate of the gravity centre corresponding to the rotation axis of the crank; V_i^{CS} and V_j^{CR} represent the volume of the crank and the conrod; I_{Ci}^{YY}, I_{Gj}^{YY} are the moment of inertia about the y-axis of the crank and the conrod; r_{CCi}, r_{GGj} are the swing arm length of the crank and the conrod; whilst m_1, m_2 and m represent as the mass of the crank, the conrod and total mass, respectively.

2.4 Structural Model

The structural model is built in order to comply with the requirements on strength, fatigue and stability of SCM structure. Diagrams representing the crank and the conrod are presented in Fig. 7.

2.4.1 Strength Limits

For the structural analysis, the crank can be considered as a beam subject to a transversal load P and an axial load N_1, while the conrod is only submitted to an axial load N_2.

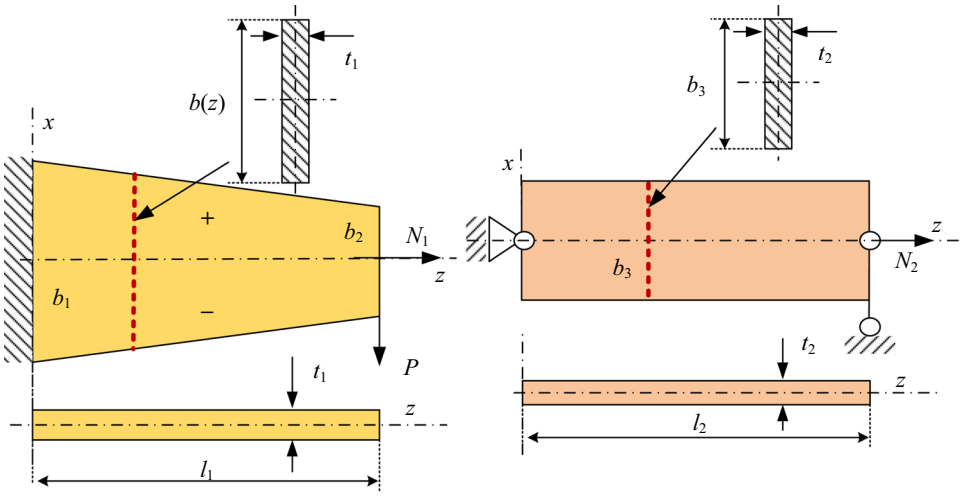

(a) Crank **(b)** Conrod

Fig. 7 Crank and conrod diagrams

(i) Strength limits of the crank and conrod are expressed by [19]:

$$\begin{cases} \dfrac{\sigma_b}{\max \sigma_1} \geq n_b \\ \dfrac{\sigma_b}{\max \sigma_2} \geq n_b \end{cases} \tag{17}$$

where n_b is the strength safety factor; σ_1 and σ_2 are normal stresses of crank and conrod, respectively, which are defined as:

$$\begin{cases} \sigma_1 = \sigma_{N_1} \pm \sigma_M = \dfrac{N_1}{A_1(z)} \pm \dfrac{M_y(z)x(z)}{J_y} = \dfrac{N_1}{A_1(z)} \pm \dfrac{M_y(z)}{W_y(z)} = \dfrac{N_1}{t_1 b(z)} \pm 6\dfrac{P(l_1 - z)}{t_1 b^2(z)} \\ \sigma_2 = \dfrac{N_2}{A_2} = \dfrac{N_2}{b_3 t_2} \end{cases} \tag{18}$$

Determination of crank cross section $A_1(z)$, compression/tension load N_1 and N_2, and load T is provided in Appendix 2.

(ii) The conditions for the crank and the conrod not fail by shear at joints O and A (Fig. 5) is that the maximum shear stress at the sections of working cycles does not exceed the critical shear stress, τ_c, complying to:

$$\begin{cases} \dfrac{\max(2\sqrt{\mathrm{XO}^2 + \mathrm{YO}^2})}{(b_1 - d_1)h_1} \leq \dfrac{\tau_c}{n_b} \\ \dfrac{\max(2\sqrt{\mathrm{XA}^2 + \mathrm{YA}^2})}{(b_2 - d_2)h_2} \leq \dfrac{\tau_c}{n_b} \\ \dfrac{\max(2\sqrt{\mathrm{XA}^2 + \mathrm{YA}^2})}{(b_3 - d_2)h_3} \leq \dfrac{\tau_c}{n_b} \end{cases} \tag{19}$$

(iii) The strength conditions for the key are expressed as follows:

$$\begin{cases} \dfrac{2(M + Tl_1)}{d_1 h_1 (h_t - t_{1t})} \leq \dfrac{\sigma_b}{n_b} \\ \dfrac{2(M + Tl_1)}{d_1 h_1 b_t} \leq \dfrac{\tau_c}{n_b} \end{cases} \tag{20}$$

where h_t, t_t, b_t are the dimensions of the key.

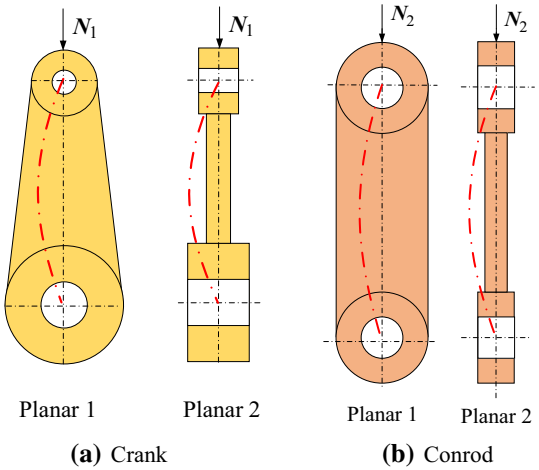

Fig. 8 Buckling of the crank and conrod in two different planes—plane of motion and a plane perpendicular to the plane of motion

2.4.2 Fatigue

Fatigue strength of the crank and conrod is expressed by [19].

$$\begin{cases} \dfrac{\sigma_{-1}}{k\sigma_\alpha + \alpha_\sigma \sigma_m} \geq n_f \\ \dfrac{\sigma_{-1}}{k \max \sigma_2} \geq n_f \end{cases} \tag{21}$$

where $\sigma_\alpha = \frac{\max \sigma_1 - \min \sigma_1}{2}$ and $\sigma_m = \frac{\max \sigma_1 + \min \sigma_1}{2}$ represent stress amplitude and average stress of the crank, respectively; k is a product of various factors that can influence the fatigue strength; and n_f is the fatigue safety factor.

2.4.3 Stability

To avoid lateral buckling of the crank, its thickness is limited by the formula $\frac{t_1}{b_1} \geq \frac{1}{10}$ [27]. Further, the condition on which the crank will be stable under axial loads N_1 and N_2, Fig. 8, should be investigated. From the theoretical point of view, instability can occur in two different planes [19]. However, with the assumed geometry for the SCM structural elements, instability of the crank and conrod will first occur on a plane perpendicular to the plane of motion

(symmetric planar 2, as shown in Fig. 8). Hence, a study on this plane is needed. Critical loads of the crank N_{cr1} and N_{cr2} are derived by using the strain energy method [28, 29].

The total potential energy $\Im$ of the crank is:

Table 1 Model parameters

	Parameter	Units	Details
Size, working space	h	m	Width limit
	b	m	Length limit
	s	m	Working trajectory
Load	m_3	kg	Slider mass (const.)
	F	N	Drag force
Power	n	(rev/min)	Angular velocity of crank
Material properties	ρ	kg/m^3	Density
	μ	–	Slider—groove coefficient of friction
	σ_b	MPa	Critical normal stress
	τ_c	MPa	Critical shear stress
	n	–	The safety factor in terms of the requirements on strength, fatigue and shear
	E	N/m^2	Elastic modulus
	σ_{-1}	MPa	Fatigue limit
	k, α_σ	–	Coefficient of material effect on oscillating feature (symmetrical and asymmetrical)

Table 2 Variable vector α

Symbol in the model	Real symbol	Units	Detail
α_1	t_1	m	The least thickness of crank
α_2	t_2	m	The least thickness of connecting rod
α_3	K	N/m	Stiffness K of spring
α_4	b_1	m	The maximum width of crank
α_5	b_2	m	The minimum width of crank
α_6	b_3	m	Width of connecting rod
α_7	d_1	m	Internal diameter of the crank upper part
α_8	d_2	m	Internal diameter of the crank lower part
α_9	h_1	m	Thickness of the crank upper part
α_{10}	h_2	m	Thickness of the crank lower part
α_{11}	h_3	m	Thickness of the connecting rod ends

Table 3 Constraints

Constraint	Detail	Expressions
f_1	Geometry of SCM	(1), (2)
f_2	Manufacturability and assembly requirements	(3), (4)
f_3	Strength limits of the crank and connecting rod	(17)
f_4	Condition for the crank and connecting rod not to be broken	(19)
f_5	Strength requirement for the key	(20)
f_6	Fatigue requirement for the crank and connecting rod	(21)
f_7	Stability requirement for the crank and connecting rod	(26)

Table 4 Criteria in the multiobjective design of an SCM structure

Criteria	Detail	Expressions
$\Phi_1 \rightarrow$ MIN	Mass of SCM	(16)
$\Phi_2 \rightarrow$ MIN	Required power	(11)
$\Phi_3 \rightarrow$ MIN	Maximum dynamic reaction at joint A	(7)

$$\Im = \frac{1}{2}\int_0^{l_1} EI(z)(y'')^2 \mathrm{d}z - \frac{N_1}{2}\int_0^{l_1}(y')^2 \mathrm{d}z \tag{22}$$

where $I(z) = \frac{b_1 t_1^3}{12}\left(\frac{l_1 - z}{l_1}\right) + \frac{b_2 t_1^3}{12}\frac{z}{l_1}$ is the moment of inertia of the crank cross section.

An approximation of function y is selected by using the boundary conditions $y(0)=0$, $y'(0)=0$, $y(l_1)=0$, $y'(l_1)=0$ as follows:

$$y = \beta\left(1 - \cos\left(\frac{2\pi z}{l_1}\right)\right) \tag{23}$$

Based on the principle Lagrange–Dirichlet, the critical load $N_{1\mathrm{cr}}$ is obtained by means of the first derivative condition of $\delta\Im = 0$.

$$N_{\mathrm{cr1}} = \frac{1}{6}\frac{\pi^2 t_1^3 E(b_1 + b_2)}{l_1^2} \tag{24}$$

On the other hand, the critical load on the conrod is derived by the formula Euler [19]:

$$N_{cr2} = \frac{\pi^2 E}{(0.5l_2)^2}\frac{b_3 t_2^3}{12} = \frac{\pi^2 E b_3 t_2^3}{3l_2^2} \tag{25}$$

Yet, the requirement that the crank and connecting rod will not be unstable is:

$$\begin{cases} \dfrac{N_{\mathrm{cr1}}}{\max N_1} \geq n_{\mathrm{st}} \\ \dfrac{N_{\mathrm{cr2}}}{\max N_2} \geq n_{\mathrm{st}} \end{cases} \tag{26}$$

where n_{st} is a buckling safety factor (commonly in the range of 5—6) [19].

3 Multiobjective Optimization Model of SCM

3.1 Generalized Mathematical Model

The above-mentioned expressions (1)–(26) can be considered as a database of the generalized model. It includes the majority of the technical factors in the design process of an SCM. However, their use varies according to each design circumstance and design engineer's perception. For instance, a designer can only bear in mind some factors and leave behind others from his subjective point of view. Doing this results in different models in terms of variables, constraints and objective functions representing quality criteria for an SCM. In this work, it is presented a generalized model including 14 parameters, 11 variables, seven constrained expressions and three objective functions. These data are set forth in Tables 1, 2, 3 and 4.

3.1.1 Parameters

The listed parameters in Table 1 are constant, among them σ_b, τ_c, E, σ_{-1}, α_σ, k are taken from the literature [19, 30].

3.1.2 Variables

The variables of the SCM structure are included in Table 2.

3.1.3 Constraints

Based on the analysis in Sect. 2, the constrained expressions for SCM structure are established and presented in detail in Table 3.

3.1.4 Objective Function

The criteria in the multiobjective design of SCM structure are provided in Table 4.

3.2 Validation of the Mathematical Model

Since the expressions (1)–(26) have been built by using classical mechanics, they are theoretically reliable. To validate the developed model, several factors are analysed in comparison with the results obtained by the finite element method (FEM). The comparative study involves a particular parameter set such as: $b_1 = 0.045$ m, $b_2 = 0.02$, $b_3 = 0.02$, $t_1 = t_2 = 0.006$ m, $h_1 = h_3 = 0.018$, $h_2 = 0.016$ m, $d_1 = 0.01$ m, $d_2 = 0.005$ m.

Figure 9 shows the stress distribution of a crank obtained by means a FEM analysis and the developed model. It can be observed that the stress distribution along the crank length from these two tools is quite similar. Yet, the model allows for the determination of stress distribution not only at a particular moment, but also for the entire cycle. Also, the stress distribution in the crank over the tine of a single cycle from the model almost coincides with the one from FEM, as it can be seen in Fig. 10.

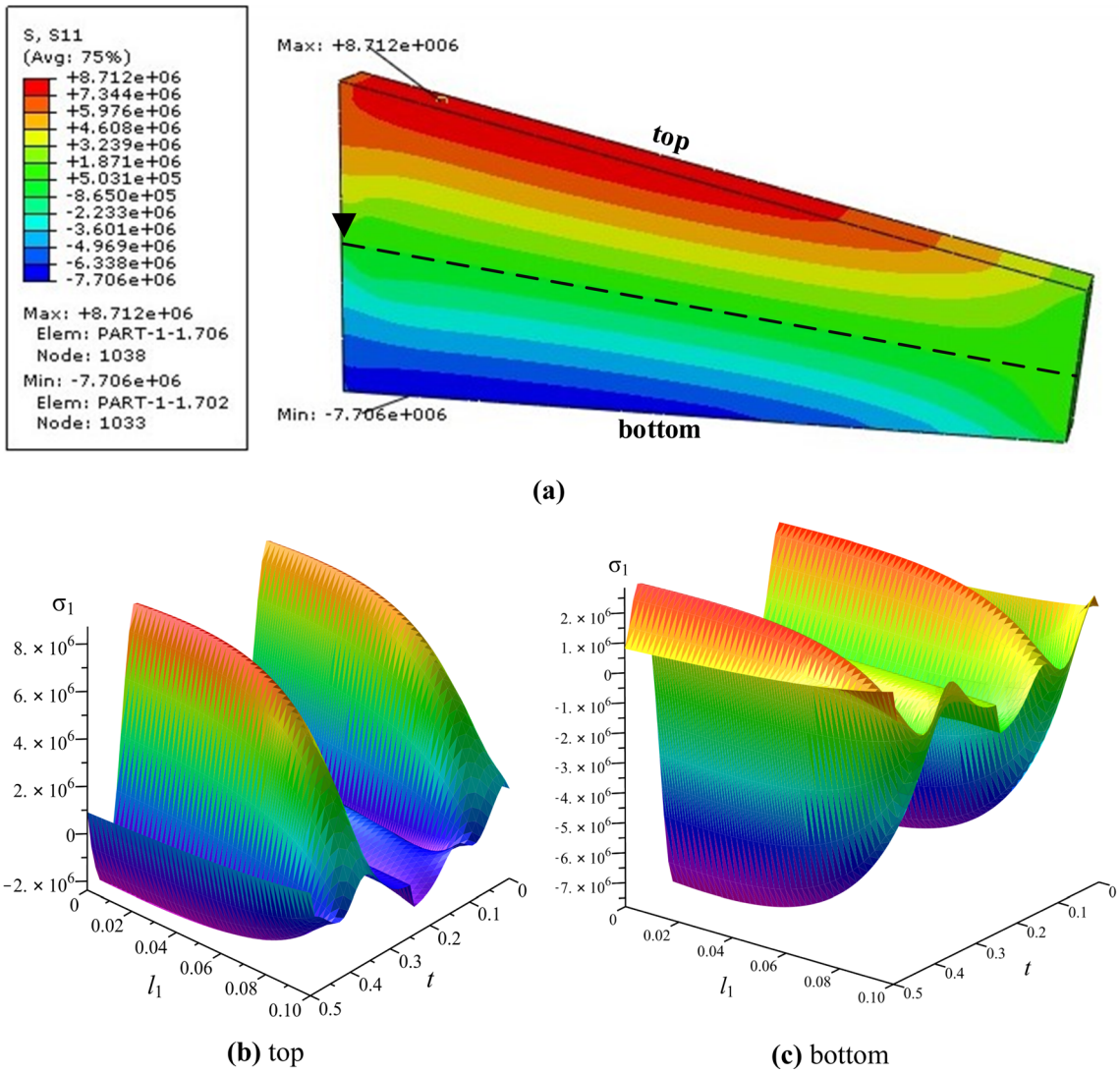

Fig. 9 Stress distribution in the crank in a single cycle. **a**—FEM; **b** and **c**—developed model

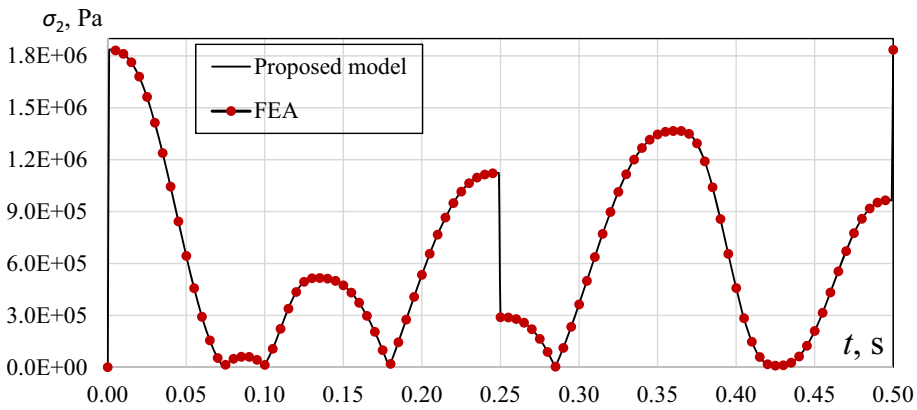

Fig. 10 Stress distribution in the crank over the time of a single cycle from the model and FEM

Table 5 Maximum stress of the crank and conrod

Value		Developed model	FEM	Deviation (%)
Crank	$\max\sigma_1$ (MPa)	8.957	8.712	2.812
	$\min\sigma_1$(MPa)	− 7.884	− 7.706	2.310
Connecting Rod	$\max\sigma_2$ (MPa)	1.835	1.835	0.0

Table 6 Critical loads on the crank and connecting rod

	Developed model	FEM	Deviation (%)
N_{cr1} (N)	461,897	426,930	4.8
N_{cr2} (N)	31,581	31,492	0.3

Table 5 provides maximum stress of crank and conrod given by the developed model and by FEM. It also reveals that the deviation is less than 3%, which is minor. Regarding critical loads N_{cr1} of crank and N_{cr2} of conrod, which are presented in Table 6, the deviation between FEM and the ones provided by the proposed model is also negligible (less than 5%). These results indicate that the model is precise and reliable.

4 Case study—Main Transmission System of Fruit and Vegetable Washer

One spring-SCM application is the main transmission system of a fruit/vegetable washer [24, 31, 32]. The spring-SCM creates a shaking motion of the washer drum, as illustrated in Fig. 11, in order to clean fruit and vegetable properly. With an experience-based approach, there is an initial variable set and an interval of variables, which are presented in Table 7.

4.1 Determination of Pareto Optimal Solutions

Based on the developed model, a genetic algorithm optimization [33] is used to determine Pareto optimal solutions. This procedure is carried out by using MATLAB, and 73 Pareto optimal solutions were found, some of which are included in Table 8. Distribution of solutions in the space of objective functions is illustrated in Fig. 12. Hence, as the number of Pareto solutions is quite large, the question of which ones should be selected for design purposes is of major concern to the analyst.

4.2 Filter of Solutions with Multiobjective Decision-Making Method

Among the aforementioned 73 Pareto optimal solutions, it is possible to filter out the suitable one based on the decision-making method. In fact, the priority order of criteria or objective functions is diversified upon the customer requirements. As soon as the priority order varies, the obtained

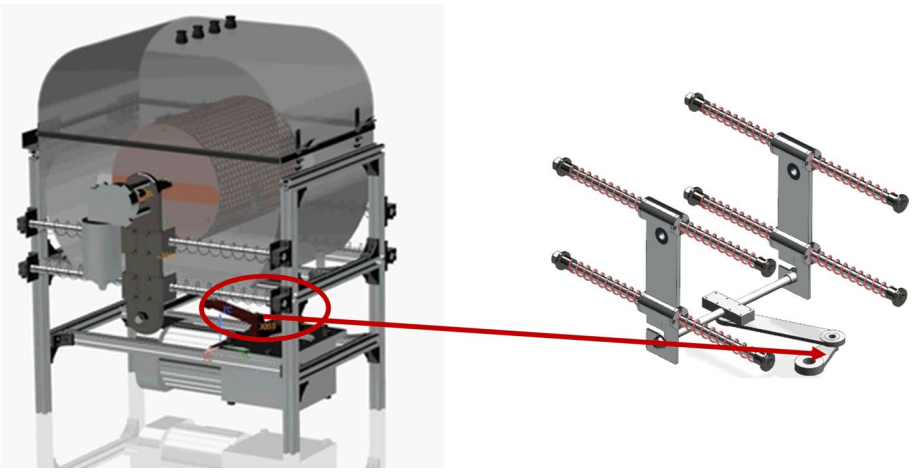

Fig. 11 Spring-SCM in the fruit and vegetable washer [23]

Table 7 Initial variable set and interval of variables

	α_1	α_2	α_3	α_4	α_5	α_6	α_7	α_8	α_9	α_{10}	α_{11}
S0	0.009	0.004	487.7	0.067	0.047	0.032	0.055	0.025	0.019	0.011	0.02
maxα	0.003	0.003	0	0.03	0.03	0.03	0.006	0.006	0.009	0.006	0.006
minα	0.03	0.03	1000	0.1	0.1	0.1	0.06	0.03	0.055	0.03	0.03

Table 8 Several available Pareto optimal solutions

No.	α_1	α_2	α_3	α_4	α_5	α_6	α_7	α_8	α_9	α_{10}	α_{11}	Φ_1	Φ_2	Φ_3
1	0.176	0.177	570.2	0.841	0.578	0.608	0.483	0.25	0.251	0.259	0.280	39.521	3.483	83.587
2	0.118	0.166	676.8	0.715	0.514	0.506	0.506	0.3	0.220	0.211	0.242	39.083	2.067	97.194
3	0.117	0.165	702.1	0.712	0.511	0.510	0.502	0.3	0.218	0.222	0.242	39.039	2.084	99.663
4	0.174	0.174	571.0	0.779	0.537	0.649	0.486	0.25	0.241	0.253	0.254	39.547	3.301	83.783
5	0.176	0.176	570.9	0.832	0.571	0.613	0.482	0.25	0.247	0.258	0.278	39.523	3.443	83.697
6	0.173	0.173	570.5	0.837	0.568	0.601	0.486	0.25	0.246	0.253	0.274	39.496	3.347	83.930
7	0.135	0.166	662.5	0.727	0.515	0.513	0.501	0.3	0.220	0.221	0.241	39.118	2.177	95.559
8	0.150	0.166	611.9	0.741	0.528	0.510	0.490	0.3	0.224	0.227	0.242	39.211	2.279	90.349
9	0.175	0.176	570.7	0.827	0.565	0.586	0.484	0.25	0.234	0.253	0.278	39.480	3.247	84.083
10	0.171	0.173	573.4	0.780	0.546	0.538	0.486	0.25	0.242	0.250	0.270	39.386	2.855	85.202
…														
64	0.153	0.166	688.2	0.767	0.530	0.512	0.499	0.3	0.226	0.236	0.244	39.071	2.355	97.873
65	0.131	0.166	665.2	0.721	0.524	0.507	0.505	0.3	0.221	0.221	0.243	39.107	2.146	95.855
66	0.176	0.174	570.7	0.832	0.568	0.574	0.487	0.25	0.246	0.254	0.279	39.458	3.230	84.216
67	0.174	0.173	571.7	0.812	0.561	0.556	0.489	0.25	0.243	0.249	0.270	39.416	3.033	84.713
68	0.143	0.166	662.2	0.739	0.521	0.509	0.499	0.3	0.220	0.235	0.252	39.122	2.255	95.368
69	0.119	0.166	646.0	0.739	0.517	0.510	0.504	0.3	0.221	0.214	0.242	39.146	2.143	94.043
70	0.177	0.173	570.2	0.762	0.522	0.637	0.486	0.25	0.237	0.249	0.276	39.559	3.265	83.726
71	0.132	0.171	593.8	0.757	0.520	0.517	0.495	0.3	0.237	0.226	0.246	39.265	2.336	88.515
72	0.162	0.095	618.5	0.797	0.489	0.436	0.414	0.25	0.204	0.249	0.188	38.779	1.144	99.558
73	0.172	0.174	574.0	0.789	0.559	0.550	0.490	0.25	0.246	0.247	0.264	39.398	2.938	85.088

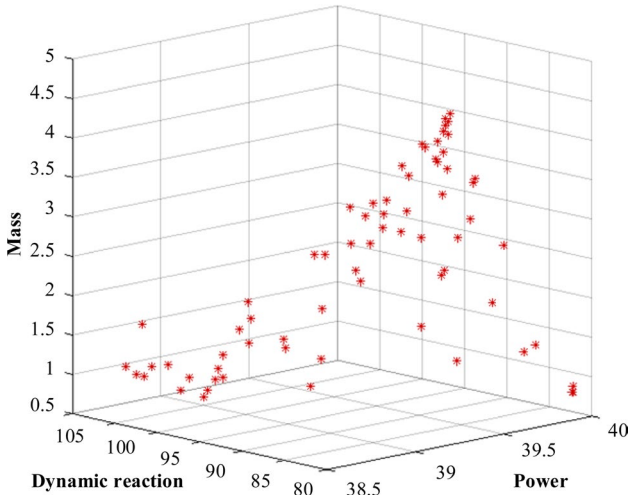

Fig. 12 Distribution of Pareto optimal solutions by GA-optimization

Table 9 Resultant solutions once the priority order of objective functions varies

Solution	Priority order	№	Φ_1	Φ_2	Φ_3
S1	$\{\Phi_1 \mapsto \Phi_2 \mapsto \Phi_3\}$	72	38.779	1.144	99.558
S2	$\{\Phi_1 \mapsto \Phi_3 \mapsto \Phi_2\}$	59	38.851	1.150	97.260
S3	$\{\Phi_2 \mapsto \Phi_3 \mapsto \Phi_1\}$	25	38.845	1.186	98.601

design option would be different. One of the most common decision-making methods for dealing with multiobjective optimization problems is the method of successive concessions [34, 35], which is used in this study. Table 9 provides three resultant solutions once the priority order of objective functions Φ1, Φ2, Φ3 varies.

5 Results

The design solutions (corresponding to solutions S1, S2, S3) obtained by the developed model are analysed in comparison with the ones (S0) from the experience-based approach, which is described in Ref. [36]. For the sake of convenience, the objective function values are established in the interval [0,1] by using the formula $\|\Phi\| = \frac{\Phi - \min \Phi}{\max \Phi - \min \Phi}$. Parameter set obtained by the experience-based approach and the developed model are presented in Table 10 and the comparative results can be observed in Table 11 and Fig. 13.

It can be observed in Table 12 and in Fig. 13 that solutions obtained by the developed model are better the one obtained by the experience-based approach, i.e. mass, required power and dynamic forces are reduced by 1–3%, 13–24% and 17–25%, respectively. Every solution S0, S1, S2 and S3 corresponds to a particular configuration of the SCM, as shown in Fig. 14.

Table 10 Parameter set obtained by the experience-based approach (S0) and the developed model (S1, S2, S3)

Solutions	t_1	t_2	K	b_1	b_2	b_3	d_1	d_2	h_1	h_2	h_3
S0	0.149	0.079	912.5	0.812	0.518	0.498	0.341	0.17	0.267	0.280	0.190
S1	0.162	0.095	618.5	0.797	0.489	0.436	0.414	0.25	0.204	0.249	0.188
S2	0.172	0.065	592.4	0.886	0.487	0.447	0.288	0.25	0.228	0.243	0.158
S3	0.117	0.166	702.1	0.712	0.511	0.510	0.502	0.30	0.218	0.222	0.242

Table 11 Comparative results

Objective function	Experience-based approach S0	Developed model		
		S1	S2	S3
Φ_1, W	40.022	39.067	39.224	39.040
Improvement of Φ_1, % (in comparison with S0)	–	– 2.39%	– 1.99%	
Φ_2, kg	2.497	1.894	2.148	2.084
Improvement of Φ_2, % (in comparison with S0)	–	– 24.14%	– 13.98%	– 16.53%
Φ_3, N	120.825	92.391	90.145	99.663
Improvement of Φ_3, % (in comparison with S0)	–	– 23.53%	– 25.39%	– 17.51%

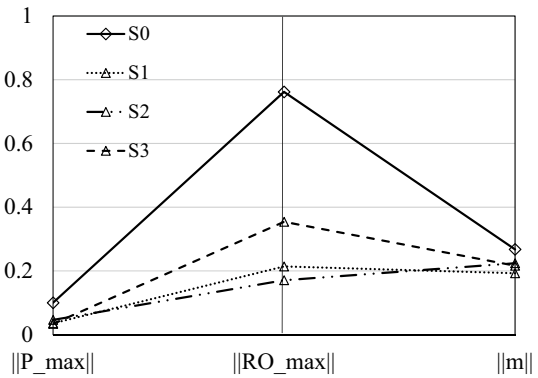

Fig. 13 Illustrative comparison of the outcome. S0—from experience-based approach [36] and S1, S2, S3- from the developed model

One solution of the three from the developed model (S1, S2, S3) was selected for the manufacture of the main transmission system of the fruit and vegetable washer, as illustrated in Fig. 15. It is noteworthy that with the developed model, the design process of the spring-SCM for the washer has become more flexible, convenient and effective. The model allows to generate a Pareto optimal set based on this the suitable optimal solutions can be selected according to specific manufacturing scenarios.

6 Conclusion

A generalized model for SCM with a spring system, in which there are 11 variables, seven constrained expressions and three objective functions is developed in this paper. Some variables were of a discrete type, which are common data of the standard components available in the market. Also, the constraint includes multiple factors of SCMs such as strength limits, fatigue and stability from the structural standpoint, geometrical conditions of the system,

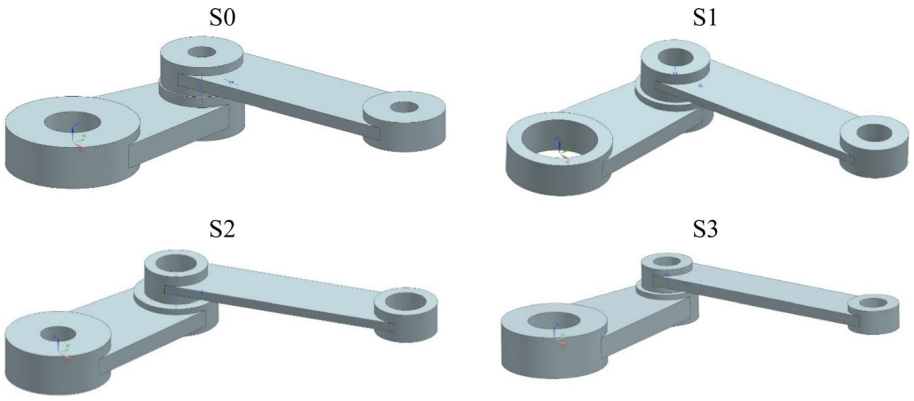

Fig. 14 3D model of SCM based on the outcome. S0, from experience-based approach [36] and S1, S2 and S3, from the developed model

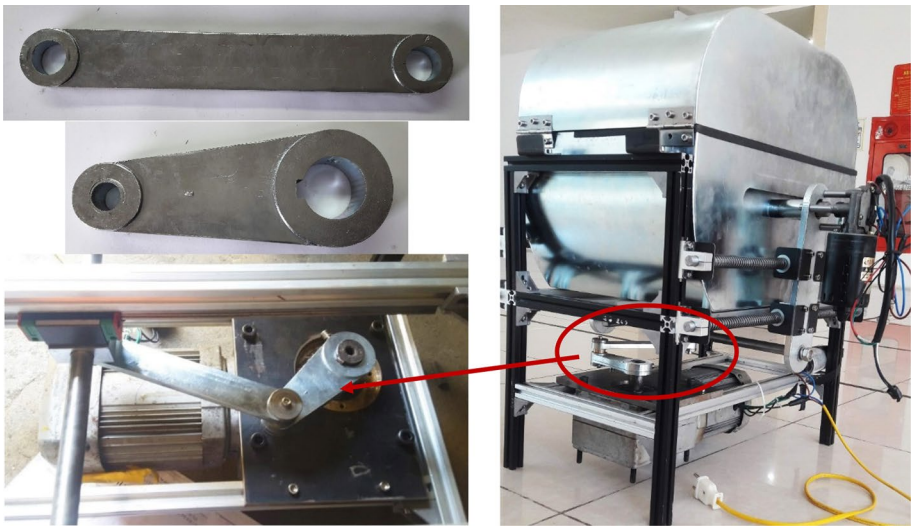

Fig. 15 Application of the spring-SCM for the fruit and vegetable washer

manufacturability and assembly requirements. The most important three criteria or objective functions are total of mass, the required driving power and the maximum dynamic support reaction. The correctness of the model was verified by means of a numerical simulation.

Next, the developed model was applied for the design process of a main transmission of the patented fruit and vegetable washer. Besides, by using the genetic algorithm optimization, 73 Pareto optimal solutions were determined. Then, with a decision-making process based on the method of successive concessions, the three most suitable optimal solutions according to the specific manufacturing scenario were defined. The comparative study showed that the solutions obtained by the developed model have excelled the one yielded by the experience-based approach. At the same time mass of SCM, the required power and maximum dynamic reaction are reduced by 1–3%, 13–24% and 17–25%, respectively. Therefore, they were implemented effectively for further manufacture of fruit/vegetable washer.

It is remarkable that, in addition to design main transmission system of the fruit/vegetable washer, the generalized mathematical model also can be used for SCM design in many kinds of mechanical system, in which there might be different numbers of variable, constraint and criteria depending upon the specific circumstance. The model would yield a reliable design parameter set without having to re-check by using the costly analysis software based on the finite element method. Besides, the multiobjective optimization problem can be solved conveniently by using the model that would save time and expenditure in an efficient manner. And last but not least, it can be seen that the approach proposed in this paper can be widely applied for design of other mechanisms.

Appendix 1

Dynamic Formulation

$\begin{cases} \varphi_{\mathrm{OA}} = \varphi = \varphi(t); \\ \omega_{\mathrm{OA}} = \omega = \dfrac{\mathrm{d}}{\mathrm{d}t}\varphi(t) = \varphi'(t); \\ \varepsilon_{\mathrm{OA}} = \varepsilon = \dfrac{\mathrm{d}^2}{\mathrm{d}t^2}\varphi(t) = \varphi''(t) \end{cases}$	Angular coordinate, velocity, acceleration of the crank
$x_A = l_1 \cos\varphi; y_A = l_1 \sin\varphi$	Joint A coordinates
$x_B = x_A + \sqrt{l_2^2 - (y_A - \Delta)^2};$ $y_B = \Delta = \mathrm{const}$	Slider B coordinates
$x_C = \cos\varphi \cdot u_C - \sin\varphi \cdot v_C;$ $y_C = \sin\varphi \cdot u_C + \cos\varphi \cdot v_C$	Gravity centre C coordinates of the crank
$\sin\theta = \frac{y_A - \Delta}{l_2};\ \cos\theta = \sqrt{1 - (\sin\theta)^2}$	Sine and cosine of the angle θ, formed by the conrod and horizontal direction as shown in Fig. 1
$\begin{cases} x_G = x_A + \cos\theta \cdot u_G + \sin\theta \cdot v_G \\ y_G = y_A - \sin\theta \cdot u_G + \cos\theta \cdot v_G \end{cases}$	Gravity centre G coordinates of the conrod
$v_{B/Cx/Cy/Gx/Gy} = \dfrac{\mathrm{d}}{\mathrm{d}t}\left(x_B/x_C/y_C/x_G/y_G\right) = f_{1\div5}(\varphi, \varphi')$	Velocity and acceleration of the slider B, gravity centres C and G, respectively
$a_{B/Cx/Cy/Gx/Gy} = \dfrac{\mathrm{d}^2}{\mathrm{d}t^2}\left(x_B/x_C/y_C/x_G/y_G\right) = f_{6\div10}(\varphi, \varphi', \varphi'')$	
$\omega_{\mathrm{AB}} = \dfrac{v_B}{\mathrm{PB}} = \dfrac{v_B}{x_B \tan\varphi - \Delta} = f_{11}(\varphi, \varphi')$	Angular velocity and acceleration of the conrod
$\varepsilon_{\mathrm{AB}} = \dfrac{\mathrm{d}}{\mathrm{d}t}\omega_{\mathrm{AB}} = f_{12}(\varphi, \varphi', \varphi'')$	

$s = \text{signum}(v_B) = \pm$	This function determines sign and direction of slider B motion at any time t. As the slider moves right hand, s possesses the sign "+" and vice versa

Appendix 2

Cross Section and Loads on the Crank and Conrod

- Cross section of the crank: $b(z) = b_1 \frac{l_1 - z}{l_1} + b_2 \frac{z}{l_1}, \quad z = 0..l_1$
- Compression/tension load on the crank: $N_1 = X_A \cdot \cos\varphi(t) + Y_A \cdot \sin\varphi(t)$
- Load orthogonal to the crank: $T = X_A \cdot \sin\varphi(t) - Y_A \cdot \cos\varphi(t)$
- Compression/tension load on the connecting rod: $N_2 = X_A \cdot \cos\theta(t) - Y_A \cdot \sin\theta(t)$

Appendix 3

Nomenclature

F External force (N)
S Cross-sectional area of drum (cm^2)

Greek Letters

η Viscosity coefficient of water (kg/m × s)
μ Friction coefficient
ρ Density of water (kg/m^3)
ω Angular velocity (rad/s

Subscripts

opt Optimized
max Maximum
min Minimum

References

1. Pandrea, N.; Popa, D.: Classical and Mmodern Aapproaches in the Ttheory of Mmechanisms, p. 433. Wiley, Hoboken (2017)
2. Varedi, S.M.; Daniali, H.M.; Dardel, M.: Dynamic synthesis of a planar slider–crank mechanism with clearances. Nonlinear Dyn. (2014). https://doi.org/10.1007/s11071-014-1762-x
3. Jomartov, A.A.; Joldasbekov, S.U.; Drakunov, Yu.M.: Dynamic synthesis of machine with slider-crank Mechanism. Mech. Sci. **6**, 35–40 (2015). https://doi.org/10.5194/ms-6-35-2015
4. Dieter, G.; Schmidt, L.: Engineering Design, 5th edn. McGraw-Hill Higher Education, New York (2012)
5. Huang, M.-S.; Chen, K.-Y.; Fung, R.-F.: Comparison between mathematical modeling and experimental identification of a spatial slider–crank mechanism. Appl. Math. Model. **34**, 2059–2073 (2010)
6. Rider, M.J.: Design and Analysis of Mechanisms: A Planar Approach, p. 315. Wiley, Hoboken (2015)
7. Ha, J.-L.; Fung, R.-F.; Chen, K.-Y.; Hsien, S.-C.: Dynamic modeling and identification of a slider-crank mechanism. J. Sound Vib. **289**, 1019–1044 (2006)
8. Akbari, S.; Fallahi, F.; Pirbodaghi, T.: Dynamic analysis and controller design for a slider–crank mechanism with piezoelectric actuators. J. Comput. Des. Eng. **3**(4), 312–321 (2016)
9. Groza, D.: Balancing of a slider-crank mechanism by using a counter mass and a progressive spring with two rates. Appl. Mech. Mater. **823**, 37–42 (2016)
10. Arakelian, V.; Briot, S.: Simultaneous inertia force/moment balancing and torque compensation of slider-crank mechanisms. Mech. Res. Commun. **37**, 265–269 (2010)
11. Daniel, G.B.; Cavalca, K.L.: Analysis of the dynamics of a slider–crank mechanism with hydrodynamic lubrication in the connecting rod–slider joint clearance. Mech. Mach. Theory **46**, 1434–1452 (2011)
12. Li, Y.; Chen, G.; Sun, D.; Gao, Y.; Wang, K.: Dynamic analysis and optimization design of a planar slider–crank mechanism with flexible components and two clearance joints. Mech. Mach. Theory **99**, 37–57 (2016)
13. Chen, Y.; Sun, Y.; Chen, C.: Dynamic analysis of a planar slider-crank mechanism with clearance for a high speed and heavy load press system. Mech. Mach. Theory **98**, 81–100 (2016)
14. Khemili, I.; Abdallah, M.A.B.; Aifaoui, N.: Multiobjective optimization of a flexible slider-crank mechanism synthesis, based on dynamic responses. Eng. Optim. (2018). https://doi.org/10.1080/0305215X.2018.1508574
15. Mariti, L., et al.: Optimization of a High-speed deployment slider-crank mechanism: a design charts approach. J. Mech. Des. (2014). https://doi.org/10.1115/14025702
16. Azegami, H.; Zhou, L.; Umemura, K.; Kondo, N.: Shape optimization for a link mechanism. Struct. Multidisc. Optim. **48**, 115–125 (2013)
17. Chaudhary, K.; Chaudhary, H.: Optimal design of planar slider-crank mechanism using teaching-learning-based optimization algorithm. J. Mech. Sci. Technol. **29**(12), 5189–5198 (2015)
18. Conte, F.L.; George, G.R.; Mayne, R.W.; Sadler, J.P.: Optimum mechanism design combining kinematic and dynamic-force considerations. J. Eng. Ind. **97**(2), 662–670 (1975). https://doi.org/10.1115/1.3438631
19. Bhandari, V.B.: Design of Machine Elements, 3rd edn., p. 934. Tata McGraw-Hill Education, New York (2010)
20. Ullman, D.G.: The Mechanical Design Process, 4th edn., p. 433. McGraw-Hill Higher Education, New York (2010)
21. Ilhami, M.A.; Masruroh, N.A.: A mathematical model at the detailed design phase in the 3DCE new product development. Comput. Ind. Eng. (2020). https://doi.org/10.1016/j.cie.2020.106617
22. Shidpour, H.; Shahrokhi, M.; Bernard, A.: A multi-objective programming approach, integrated into the TOPSIS method, in order to optimize product design; in three-dimensional concurrent engineering. Comput. Ind. Eng. **64**(4), 875–885 (2013)
23. Dang, H.M.; Phung, V.B.; Nguyen, V.D.; Tran, T.T.: Multifunctional fruit and vegetable washer. VN Patent Application № VN2019324A2 (2019) (in submission)

24. Dang, H.M.; Bui, V.P.; Phung, V.B.; Nguyen, V.D.: Design, development and performance evaluation of a new-type fruit vegetable washer. J. Mech. Eng. Res. Dev. **43**(4), 265–274 (2020)
25. Nguyen, T.T.N.; Dang, H.M., et al.: Dynamic analysis and multi-objective optimization of slider-crank mechanism for an innovative fruit and vegetable washer. J. Mech. Eng. Res. Dev. **43**(2), 127–143 (2020)
26. Favorin, M.V.: Momenty inertsii tel, Spravochnik. Mashinostroyeniye, p 312, 1970
27. Bazant, Z.P.; Cedolin, L.: Stability of Structures. World Scientific Publishing, Singapore (2010)
28. Phung, V.B.; Dang, H.M.; Gavriushin, S.S.; Nguyen, V.D.: Boundary of stability region of a thin-walled beam under complex loading condition. Int. J. Mech. Sci. **122**, 355–361 (2017)
29. Van Binh, P.; Duc, N.V.; Sergeevich, P.V.; Minh, D.H.: Improved Generalized procedure for determining critical state of a thin-walled beam under combined symmetric loads. Int. J. Struct. Stab. Dyn. **19**(8), 1950098 (2019)
30. Anuryev, V.I.: Spravochnik Konstruktora Mashinostroitelya, p. 728. Mashinostroyeniye, Moscow (1978)
31. Phuong, B.V.; Gavriushin, S.S.; Minh, D.H.; Binh, P.V.; Duc, N.V.: Application of a novel model "requirement—object—parameter" for design automation of complex mechanical system, Advances in Intelligent Systems and Computing, Springer, pp 375–384 (2020)
32. Dang, H.M., et al.: PAMMS—Procedure for Automation of Mathematical Modeling and Solution of Mechanical System: application for the design of an innovative fruit and vegetable washer. J. Mech. Eng. Res. Dev. **43**(3), 417–430 (2020)
33. Olive, K.: Genetic Algorithm Essentials. Springer, Berlin (2017)
34. Minh, D.H.; Van Binh, P.H.U.N.G.; Van Phuong, B.; Duc, N.V.: Multi-criteria design of mechanical system by using visual interactive analysis tool. J. Eng. Sci. Technol. **14**(3), 1187–1199 (2019)
35. Podinovskaya, O.V.; Podinovski, V.V.: Criteria importance theory for multicriterial decision making problems with a hierarchical structureá. Eur. J. Oper. Res. **258**(3), 983–992 (2017)
36. Bui, V.P.; Gavriushin, S.S.; Phung, V.B.; Dang, H.M.; Prokopov, V.S.: Dynamic and stress analysis of the main drive system in design process of an innovative fruit-vegetable washer. Eng. J. Sci. Innov. (2020). https://doi.org/10.18698/2308-6033-2020-4-1970